THE JOURNAL OF PHYSICAL CHEMISTRY Letters

Letter

pubs.acs.org/JPCL

Realizing Ultrafast Electron Pulse Self-Compression by Femtosecond Pulse Shaping Technique

Yingpeng Qi,[†] Minjie Pei,[†] Dalong Qi,[†] Yan Yang,[†] Tianqing Jia,[†] Shian Zhang,[*,†,‡] and Zhenrong Sun[*,†]

[†]State Key Laboratory of Precision Spectroscopy, East China Normal University, 3663 North Zhongshan Road, Shanghai 200062, China

[‡]NYU-ECNU Institute of Physics at NYU Shanghai, 3663 North Zhongshan Road, Shanghai, 200062, China

ABSTRACT: Uncorrelated position and velocity distribution of the electron bunch at the photocathode from the residual energy greatly limit the transverse coherent length and the recompression ability. Here we first propose a femtosecond pulse-shaping method to realize the electron pulse self-compression in ultrafast electron diffraction system based on a point-to-point space-charge model. The positively chirped femtosecond laser pulse can correspondingly create the positively chirped electron bunch at the photocathode (such as metal−insulator heterojunction), and such a shaped electron pulse can realize the self-compression in the subsequent propagation process. The greatest advantage for our proposed scheme is that no additional components are introduced into the ultrafast electron diffraction system, which therefore does not affect the electron bunch shape. More importantly, this scheme can break the limitation that the electron pulse via postphotocathode static compression schemes is not shorter than the excitation laser pulse due to the uncorrelated position and velocity distribution of the initial electron bunch.

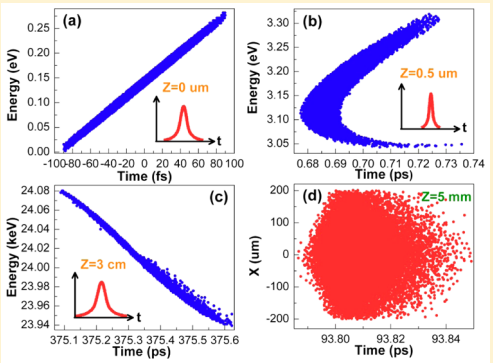

Probing ultrafast dynamical process of matter using ultrashort electron pulse with 30−300 keV can provide a 4D picture of atoms in motion,[1−3] which is based on the picometer-scale de Broglie wavelength of electrons that is ten times shorter than atomic distance and the high temporal resolution of the femtosecond laser technique. The 4D probe in time and space is realized by a pump−probe technique, where the femtosecond laser pulse is used as pump pulse and triggers the atomic motion, and the ultrashort electron pulse is used as probe pulse and measures the atomic motion status in each moment. Recently, such a pump−probe technique has shown to be well-established tool to observe complex nonequilibrium pathways through intermediate and transitional structures.[4−7]

In general, the temporal resolution in this pump−probe technique is determined by the femtosecond laser pulse duration, the electron packet duration, and their relative timing jitter.[8−10] Nowadays, the optical pulse with the duration of <10 fs from ultraviolet to near-infrared region can be directly obtained from commercial Ti:sapphire laser system, and the extreme ultraviolet attosecond pulse by high-harmonic generation can also be experimentally realized;[11,12] therefore, the temporal resolution is only limited by the electron pulse duration and the relative timing jitter. Coulomb repulsion between electrons will cause the electron pulse stretch, which will greatly affect the temporal resolution in ultrafast electron diffraction system. So far, several schemes have been proposed to compress the electron pulse.[13−24] In the case of single electron pulse without space charge effect, the single electron pulse duration is related to the initial emission energy spread,[13,14] that is, initially residual energy from photoemission, and therefore it is proportional to laser pulse width. Using radiofrequency (RF) compression technique and laser-microwave synchronization, the single electron pulse duration in the theory can be compressed to attosecond duration.[15] In the case of the multiple electron pulse, utilizing keV electron energy combined with RF compression and 3D ellipsoidal distribution of charge can obtain sub-100 fs electron pulse,[16−18] but the electron pulse duration is limited by the inevitable timing jitter.[19] Moreover, the high-energy electron pulse with MeV by RF acceleration cavity can also be shorter than 100 fs due to the complete suppression of Coulomb repulsion in the relativistic regime.[20−22] In addition, Shortening the propagation distance between the photocathode and sample and decreasing the electron density can further suppress the electron pulse broadening due to reducing the Coulomb repulsion and its action time.[23,24]

On the basis of the conservation of volume in phase space, the multielectron bunch via postphotocathode static compression schemes cannot be shorter than the initial laser pulse due to uncorrelated position and velocity distribution of the electron bunch at the photocathode from residual energy;[13,16,25,26] therefore, it greatly limits the recompression ability of the electron pulse in the subsequent propagation process. In this work, we first propose a new scheme to realize the electron pulse self-compression in the ultrafast electron

Received: June 19, 2015
Accepted: September 8, 2015

DOI: 10.1021/acs.jpclett.5b01305
J. Phys. Chem. Lett. 2015, 6, 3867−3872

diffraction system by properly designing the femtosecond laser pulse shape. The positively chirped femtosecond laser pulse can correspondingly create the initial electron bunch with the similar temporal shape at the photocathode (such as metal−insulator heterojunction), and the positively chirped electron pulse can obtain the self-compression in the subsequent propagation process due to the energy chirp and Coulomb repulsion. We show that our proposed scheme can obtain such an electron pulse being shorter than the initial laser pulse, which breaks the previously mentioned compression limitation due to uncorrelated position and velocity distribution of the initial electron bunch. Furthermore, our proposed scheme does not introduce additional components into the ultrafast electron diffraction system and therefore does not affect the electron bunch shape.

The normal electron bunch at the photocathode produced by the transform-limited femtosecond laser pulse will be stretched in time due to the Coulomb repulsion (i.e., space charge effect) in the subsequent propagation process,[9,27,28] which results in the acceleration of the leading electrons and the deceleration of the trailing ones; such a process is called a negatively chirped electron pulse. If the positively chirped electron bunch at the photocathode can be created, that is, the leading electrons with lower energy while the trailing ones with higher energy, such an electron bunch can self-compress by the Coulomb repulsion in the subsequent propagation process, the leading electrons with low velocity are accelerated while the trailing ones with high velocity are decelerated, and finally the leading and trailing electrons will have the same velocity at a specific propagation distance, and thus the electron bunch can be maximally compressed at this position. On the basis of such an idea, we propose a femtosecond pulse-shaping technique to produce the positively chirped electron bunch at the photocathode and consequently realize the electron pulse self-compression in the subsequent propagation process. Our theoretical scheme is illustrated in Figure 1; here a pulse-shaping (PS) system is introduced in front of the ultrafast electron diffraction system, which is used to produce the positively chirped femtosecond laser pulse. The positively chirped femtosecond laser pulse can correspondingly create the positively chirped electron bunch at the photocathode (such as metal−insulator heterojunction), that is to say, the electron pulse will copy the characterization of the femtosecond laser pulse, involving the pulse duration and energy chirp, and the shaped electron pulse with positive chirp can self-compress in the drift region through the acceleration field due to the energy chirp and Coulomb repulsion.

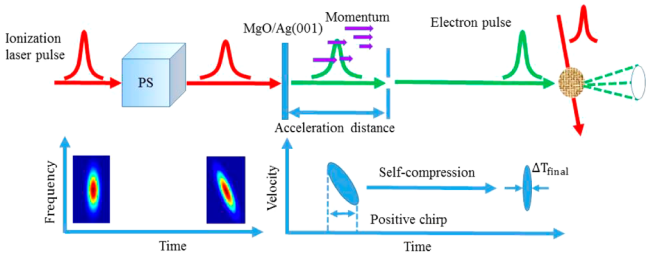

Figure 1. Proposed scheme for realizing the ultrafast electron pulse self-compression by a femtosecond pulse shaping method. The positively chirped femtosecond laser pulse obtained from a pulse shaping (PS) system excites the photocathode material (such as metal−insulator heterojunction MgO/Ag(001)) and produces the initial electron bunch with the positive chirp rate, and this chirped electron pulse can self-compress in the subsequent propagation process.

In our simulation, the propagation process of electron bunch is simulated by calculating the trajectory of individual electron in the acceleration field and drift region based on general particle tracer (GPT) software.[29] The space charge force is calculated by point-to-point Coulomb interaction and here without any approximation is taken. Furthermore, the image charge force and the electrode structure are neglected because of the strong acceleration field and relatively low electron density. In our calculation, these initial parameters are set as follows. The initial electron bunch has the Gaussian shape in time and space, and its pulse durations (full width at half-maximum (fwhm)) without and with the chirp are Δt = 20 and 60 fs, respectively. The electron number in each electron bunch is set to be N = 20 000. The radius of the electron bunch (root-mean-squared (RMS)) in the transverse direction is σ_x = 80 μm. The excess energy (i.e., residual energy) is E_{exc} = 0.1 eV and its energy spread (fwhm) is E_{spr} = 0.08 eV. The acceleration field gradient is E_{acc} = 6.86 Mv/m, and its distance is d = 3.5 mm. These main parameters and their initial values in our simulation are shown in Table 1. Here we mainly explore the effects of the initially chirped electron pulse duration, Δt, the electron number per bunch, N, the initial excess energy spread, E_{spr}, the acceleration field gradient, E_{acc}, and the acceleration field distance, d, on the electron pulse self-compression in the subsequent propagation process. These initial values in Table 1 are kept unchanged unless specific statement. Exploring the influence of these parameters is helpful to understand the physical mechanism of the chirped electron pulse self-compression and can obtain the feasible parameters in the real experiment.

Table 1. Main Parameters in Our Simulation and Their Initial Values

electron number per pulse N	20 000
radius σ_x (RMS)	80 μm
normal pulse duration Δt (fwhm)	20 fs
chirped pulse duration Δt (fwhm)	60 fs
excess energy E_{exc}	0.1 eV
excess energy spread E_{spr} (fwhm)	0.08 eV
acceleration field gradient E_{acc}	6.86 MV/m
acceleration field distance d	3.5 mm

The evolution of the positively chirped electron pulse in the subsequent process is shown in Figure 2, and here the energy spread (i.e., eV) in Y axis is used to show the electron velocity distribution in the initial and propagation processes. Utilizing the positively chirped femtosecond laser pulse to excite the photocathode material (such as metal−insulator heterojunction), these electrons with low energy emit first and then those with high energy generate, and thus the initial electron pulse at the photocathode has the similar chirp rate of the shaped femtosecond laser pulse, as shown in Figure 2a. Here the photoionization quantum efficiencies for all laser frequency components in the ultrathin metal−insulator heterojunction can be considered to be the same by the near- or below-threshold single-photon photoionization.[14] One can see that the electron pulse duration is stretched to Δt = 60 fs from 20 fs, but the electron velocity distribution keeps unchanged because the electron energy spread depends on the femtosecond laser spectral bandwidth, and this phenomenon is similar to the

DOI: 10.1021/acs.jpclett.5b01305
J. Phys. Chem. Lett. 2015, 6, 3867−3872

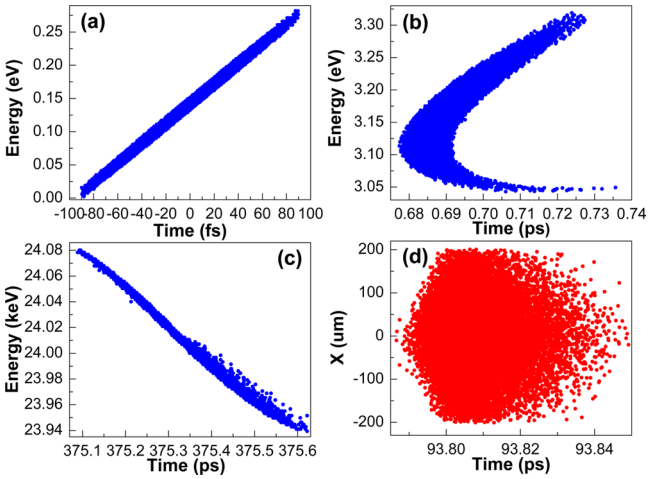

Figure 2. Distribution of the electron pulse with the excess energy spread of E_{spr} = 0.1 eV in the time for the initially chirped pulse shape at the photocathode (a), self-compressed pulse shape at the propagation distance of 0.5 μm (b), and stretched pulse shape at the propagation distance of 3 cm (c), together with the distribution of this electron pulse in the time and space at the propagation distance of 5 mm (d).

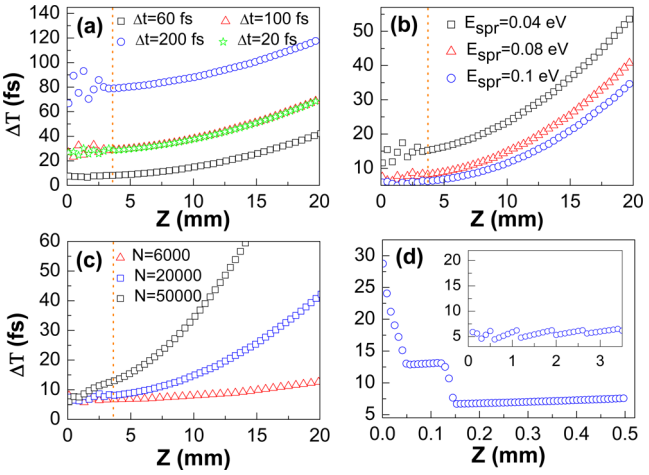

Figure 3. Dependence of the electron pulse duration evolution ΔT on the initially chirped electron pulse duration, Δt (a), excess energy spread, E_{spr} (b), and electron number per bunch, N (c), together with the electron pulse duration evolution ΔT in the acceleration field region with the excess energy spread of E_{spr} = 0.1 eV (d). The orange line is used to separate the acceleration field (left panel) and drift regions (right panel).

chirped femtosecond laser pulse. In this case, one can see that the leading electrons are with the low energy, while the trailing electrons are with the high energy. Leaving the photocathode for a short distance of 0.5 μm, the electron pulse can self-compress to a shorter duration due to the effects of the acceleration field, energy chirp and Coulomb repulsion, as shown in Figure 2b. Compared with the electron bunch at the photocathode (see Figure 2a), the electron energy distribution at this position is greatly compressed, and the leading electrons are those with the middle energy. When the compressed electron pulse continuously propagates in the acceleration field and drift regions, it will be stretched again, as shown in Figure 2c. The electron energy distribution is obviously broadened, and the leading electrons are with high energy while the trailing electrons are with low energy, which is opposite to the initial electron pulse at the photocathode (see Figure 2a). Figure 2d shows the electron bunch shape in the transverse direction (X axis) after the propagation distance of 5 mm from the photocathode. It can be seen that the compressed electron bunch can keep the Gaussian shape in the space, that is to say, the electron bunch shape in the subsequent propagation process is not affected by the chirp rate of the initial electron pulse at the photocathode, which is very important for the further applications of the compressed electron pulse in various related fields.

The initial status for the chirped electron bunch at the photocathode, such as the initial electron pulse duration, Δt, the initial excess energy spread, E_{spr}, and the initial electron number, N, is very important for realizing the electron pulse self-compression in the subsequent propagation process; therefore, next we explore the influence of these parameters on the ultrafast electron pulse self-compression. The electron pulse shape in the subsequent propagation process is not the complete Gaussian distribution, and so we utilize the standard deviation value, ΔT, to represent the electron pulse duration evolution.[8,17] Figure 3a shows the effect of the initially chirped electron pulse duration, Δt, on the electron pulse duration evolution during the propagation process. Here the horizontal axis "Z" represents the propagation distance from the photocathode, and the orange line is used to separate the acceleration field (left panel) and drift regions (right panel); hereafter the same method is utilized. As can be seen, with the increase in the initially chirped electron pulse duration from Δt = 20 to 200 fs, the electron pulse duration in the drift region first decreases and then increases, and the electron pulse is greatly compressed with the initially chirped electron pulse of Δt = 60 fs. Interestingly, the compressed electron pulse duration with ΔT = 8 fs, corresponding to the pulse duration of about Δt = 15 fs at full width at half maximum (FWHM), can be shorter than the initial electron pulse duration without the chirp rate or the transform-limited femtosecond laser pulse width (i.e., Δt = 20 fs), which breaks the compression limitation that the electron pulse is not shorter than the excitation laser pulse due to the uncorrelated position and velocity distribution of the initial electron bunch at the photocathode. It is obvious that utilizing the femtosecond pulse-shaping technique to produce the chirped electron pulse at the photocathode can provide a very important tool to realize the ultrafast electron pulse self-compression. Figure 3b presents the electron pulse duration evolution by varying the excess energy spread from E_{spr} = 0.04, 0.08 to 0.1 eV; here the corresponding excess energies are E_{exc} = 0.05, 0.1, and 0.135 eV, respectively. One can see that the electron pulse duration decreases with the increase in the excess energy spread, which is mainly due to the larger energy difference between the leading and trailing electrons, and this energy difference (i.e., velocity difference) can compensate the electron pulse broadening due to the Coulomb repulsion. Figure 3c shows the dependence of the electron pulse duration evolution on the initial electron number, N. As can be seen, the electron pulse duration increases with the increase in the initial electron number, which mainly results from the larger Coulomb repulsion for the greater electron number in the same electron bunch. On the basis of the previous observation, it can be concluded that increasing the excess energy spread and decreasing the initial electron number for a given initial electron pulse duration are a feasible scheme to obtain the shorter electron pulse.

DOI: 10.1021/acs.jpclett.5b01305
J. Phys. Chem. Lett. 2015, 6, 3867−3872

To further clearly observe the electron pulse self-compression, we present the electron pulse evolution in the acceleration field region in the case of the excess energy spread of E_{spr} = 0.1 eV, as shown in Figure 3d. It can be seen that the electron pulse is maximally compressed in the very short propagation distance and then remains almost the same duration until out of the acceleration field (see the inset of Figure 3d). Furthermore, it is noteworthy that a plateau near the propagation distance of Z = 0.1 μm is observed. We believe that this evolution behavior should be attributed to the competitive result of the acceleration field, energy chirp, and Coulomb repulsion, where both the acceleration field and Coulomb repulsion will stretch the electron pulse, while the energy chirp can compress the electron pulse. The two opposite behaviors reach a balance around the propagation distance of Z = 0.1 μm, which leads to the observation of the plateaus in Figure 3d.

As shown in Figure 3, the positively chirped electron pulse can generate the self-compression in the drift region, and even the compressed electron pulse is shorter than the initial laser pulse, but the ultrafast electron pulse self-compression only can be obtained in a relatively short propagation distance, which may lead to the great difficulty for experimental realization. To realize the electron pulse self-compression in a relatively long drift region, we propose a scheme to achieve it by varying the acceleration field distance and gradient, and the simulated results are shown in Figure 4. As can be seen in Figure 4a,

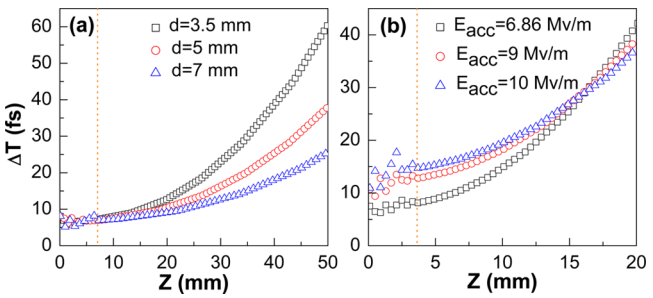

Figure 4. Dependence of the electron pulse duration evolution, ΔT, on the acceleration field distance, d (a), and gradient, E_{acc} (b), with the electron number per bunch of N = 6000.

increasing the acceleration field distance d can greatly suppress the electron pulse broadening, and such a sub-50 fs electron pulse is easy to be obtained at the propagation distance of z = 4 cm in the drift region with the acceleration field distance of d = 7 mm. With the development of machining technology, the compact ultrafast electron diffraction setup has been experimentally demonstrated.[30] Furthermore, additional components are not introduced to recompress the electron pulse, and therefore the compressed electron pulse by our proposed scheme will be high stability, which is very useful for its further applications. As can be seen in Figure 4b, increasing the acceleration field gradient E_{acc} will increase the electron pulse duration in the short propagation distance of z < 1.5 cm but decrease it in the long propagation distance of z > 1.5 cm. This observation can be attributed to the larger acceleration field gradient that results in the higher electron velocity and the weaker Coulomb repulsion in the acceleration field region, and thus the higher electron velocity will result in the slower electron pulse broadening in the same propagation distance. On the basis of such an evolution behavior in Figure 4b, one can consider two-stage acceleration fields. The first stage acceleration field with low field gradient is used to produce the maximally compressed electron pulse, while the second stage acceleration field with the high field gradient is used to slow down the electron pulse broadening, and this scheme is similar to the design of ultracold electron source[31] or high brightness electron source.[32]

We have theoretically shown that the femtosecond pulse shaping method can realize the ultrafast electron pulse self-compression in the subsequent propagation process, and the electron pulse can be compressed to be shorter than the initial laser pulse, as shown in Figures 3 and 4. In principle, this regime is similar to the compression of pulsed atom beams based on different frequency components from the femtosecond laser pulse.[33] Finally, we analyze the feasibility of our proposed scheme in real experiment. Here two important issues for our scheme must be addressed: one is to obtain the shaped femtosecond laser pulse, and the other is to produce the chirped electron pulse at the photocathode. With the progress of ultrafast pulse shaping technique, such a shaped femtosecond laser pulse with almost arbitrary temporal distribution can be obtained by a programmable 4f-configuration zero-dispersion pulse shaper combined with a 1D liquid-crystal spatial light modulator,[34] and the positively chirped femtosecond laser pulse can be generated by a quadric phase modulation in the frequency domain. To realize the positively chirped electron pulse generation at the photocathode by the positively chirped femtosecond laser pulse excitation, two conditions should be satisfied. One is that the photoelectron residual energy mainly derives from the femtosecond laser pulse and is related to the laser spectral components; the higher laser frequency can create the higher photoelectron residual energy. The other one is that the photoelectron residual energy mainly distributes on the longitudinal direction; that is to say, the photoelectrons have a preferred forward emission, which is consistent with the acceleration field direction. Recently, the metal−insulator heterojunction MgO/Ag(001) (or sandwich structure) has been shown to be a potential photocathode material to generate the high brightness electron pulse.[35,36] In this method, the photoelectron residual energy can mainly come from the femtosecond laser pulse by near- or below-threshold photoemission,[14,36] where the photon energies from different laser spectral components will be added to the electrons along the normal direction to the material surface by the direct optical transition,[35−37] and the photoelectrons can be redirected along the surface normal by varying the number of oxide layers because the reshaped surface band structure from the heterojunction can reduce the transverse energy spread at the Fermi level; that is to say, these photoelectrons mainly propagate in the longitudinal direction. Obviously, utilizing the metal−insulator heterojunction as the photocathode material can completely satisfy the two conditions in our proposed model, and the positively chirped femtosecond laser pulse can correspondingly create the positively chirped electron pulse in the metal−insulator heterojunction by the photoionization.

In summary, we have presented a new scheme to realize the ultrafast electron pulse self-compression by shaping the femtosecond laser pulse based on a point-to-point space-charge model. The positively chirped femtosecond laser pulse can correspondingly create the positively chirped electron bunch at the photocathode (such as metal−insulator heterojunction), and such a chirped electron pulse can self-compress in the

DOI: 10.1021/acs.jpclett.5b01305
J. Phys. Chem. Lett. 2015, 6, 3867−3872

subsequent propagation process. We analyzed the influence of various parameters in the ultrafast electron diffraction system on the electron pulse duration evolution in the drift region, such as the initially chirped electron pulse duration, initially residual energy spread, electron number per bunch, and acceleration field distance and gradient, and showed that such a compressed electron pulse that is shorter than the initial laser pulse can be obtained. Utilizing our proposed scheme, no additional components were introduced into the ultrafast electron diffraction system; therefore, the electron bunch shape was not affected. Furthermore, the limitation that the electron pulse is longer than the laser pulse due to the uncorrelated position and velocity distribution of the initial electron bunch at the photocathode can also be broken by our scheme. Our research presents a clear physical picture for the electron pulse self-compression in the propagation process, which is very useful for experimental design in the future.

AUTHOR INFORMATION

Corresponding Authors

*S.Z.: E-mail: sazhang@phy.ecnu.edu.cn.
*Z.S.: E-mail: zrsun@phy.ecnu.edu.cn.

Notes

The authors declare no competing financial interest.

ACKNOWLEDGMENTS

This work was partially supported by National Natural Science Fund (nos. 51132004 and 11474096) and Shanghai Municipal Science and Technology Commission (no. 14JC1401500)

REFERENCES

(1) Siwick, B. J.; Dwyer, J. R.; Jordan, R. E.; Miller, R. J. D. An Atomic-Level View of Melting Using Femtosecond Electron Diffraction. *Science* **2003**, *302*, 1382−1385.

(2) Ruan, C. − Y.; Lobastov, V. A.; Vigliotti, F.; Chen, S.; Zewail, A. H. Ultrafast Electron Crystallography of Interfacial Water. *Science* **2004**, *304*, 80−84.

(3) Nie, S.; Wang, X.; Park, H.; Clinite, R.; Cao, J. Measurement of the Electronic Grüneisen Constant Using Femtosecond Electron Diffraction. *Phys. Rev. Lett.* **2006**, *96*, 025901.

(4) Harb, M.; et al. Electronically Driven Structure Changes of Si Captured by Femtosecond Electron Diffraction. *Phys. Rev. Lett.* **2008**, *100*, 155501.

(5) Schafer, S.; Liang, W.; Zewail, A. H. Structural Dynamics and Transient Electric-Field Effects in Ultrafast Electron Diffraction from Surfaces. *Chem. Phys. Lett.* **2010**, *493*, 11−18.

(6) Schäfer, S.; Liang, W.; Zewail, A. H. Primary Structural Dynamics in Graphite. *New J. Phys.* **2011**, *13*, 063030.

(7) Gao, M.; et al. Mapping Molecular Motions Leading to Charge Delocalization with Ultrabright Electrons. *Nature* **2013**, *496*, 343−346.

(8) van Oudheusden, T.; et al. Electron Source Concept for Single-Shot Sub-100 fs Electron Diffraction in the 100 keV Range. *J. Appl. Phys.* **2007**, *102*, 093501.

(9) Gahlmann, A.; Tae Park, S.; Zewail, A. H. Ultrashort Electron Pulses for Diffraction, Crystallography and Microscopy: Theoretical and Experimental Resolutions. *Phys. Chem. Chem. Phys.* **2008**, *10*, 2894−2909.

(10) Gao, M.; Jiang, Y.; Kassier, G. H.; Miller, R. J. D. Single Shot Time Stamping of Ultrabright Radio Frequency Compressed Electron Pulses. *Appl. Phys. Lett.* **2013**, *103*, 033503.

(11) Brabec, T.; Krausz, F. Intense Few-Cycle Laser Fields: Frontiers of Nonlinear Optics. *Rev. Mod. Phys.* **2000**, *72*, 545−591.

(12) Baum, P.; Lochbrunner, S.; Riedle, E. Tunable Sub-10-fs Ultraviolet Pulses Generated by Achromatic Frequency Doubling. *Opt. Lett.* **2004**, *29*, 1686−1688.

(13) Gliserin, A.; Apolonski, A.; Krausz, F.; Baum, P. Compression of Single-Electron Pulses with a Microwave Cavity. *New J. Phys.* **2012**, *14*, 073055.

(14) Aidelsburger, M.; Kirchner, F. O.; Krausz, F.; Baum, P. Single−Electron Pulses for Ultrafast Diffraction. *Proc. Natl. Acad. Sci. U. S. A.* **2010**, *107* (46), 19714−19719.

(15) Gliserin, A.; Walbran, M.; Baum, P. Passive Optical Enhancement of Laser-Microwave Synchronization. *Appl. Phys. Lett.* **2013**, *103*, 031113.

(16) Luiten, O. J.; van der Geer, S. B.; de Loos, M. J.; Kiewiet, F. B.; van der Wiel, M. J. How to Realize Uniform Three-Dimensional Ellipsoidal Electron Bunches. *Phys. Rev. Lett.* **2004**, *93*, 094802.

(17) van Oudheusden, T.; et al. Compression of Sub-Relativistic Space-Charge-Dominated Electron Bunches for Singleshot Femtosecond Electron Diffraction. *Phys. Rev. Lett.* **2010**, *105*, 264801.

(18) Mancini, G. F.; et al. Design and Implementation of a Flexible Beamline for fs Electron Diffraction Experiments. *Nucl. Instrum. Methods Phys. Res., Sect. A* **2012**, *691*, 113−122.

(19) Kiewiet, F. B.; Kemper, A. H.; Luiten, O. J.; Brussaard, G. J. H.; van der Wiel, M. J. Femtosecond Synchronization of a 3 GHz RF Oscillator to a Mode-Locked Ti:Sapphire Laser. *Nucl. Instrum. Methods Phys. Res., Sect. A* **2002**, *484*, 619−624.

(20) Musumeci, P.; Moody, J. T.; Scoby, C. M.; Gutierrez, M. S.; Westfall, M. Laser-Induced Melting of a Single Crystal Gold Sample by Time-Resolved Ultrafast Relativistic Electron Diffraction. *Appl. Phys. Lett.* **2010**, *97*, 063502.

(21) Li, R. K.; Musumeci, P.; Bender, H. A.; Wilcox, N. S.; Wu, M. Imaging Single Electrons to Enable the Generation of Ultrashort Beams for Single-Shot Femtosecond Relativistic Electron Diffraction. *J. Appl. Phys.* **2011**, *110*, 074512.

(22) Floettmann, K. Generation of Sub-fs Electron Beams at Few-MeV Energies. *Nucl. Instrum. Methods Phys. Res., Sect. A* **2014**, *740*, 34−38.

(23) Baum, P.; Yang, D. − S.; Zewail, A. H. 4D Visualization of Transitional Structures in Phase Transformations by Electron Diffraction. *Science* **2007**, *318*, 788−792.

(24) Hebeisen, C. T.; et al. Grating Enhanced Ponderomotive Scattering for Visualization and Full Characterization of Femtosecond Electron Pulses. *Opt. Express* **2008**, *16*, 3334−3341.

(25) Fill, E.; Veisz, L.; Apolonski, A.; Krausz, F. Sub-fs Electron Pulses for Ultrafast Electron Diffraction. *New J. Phys.* **2006**, *8*, 272.

(26) Baum, P. On the Physics of Ultrashort Single-Electron Pulses for Time-Resolved Microscopy and Diffraction. *Chem. Phys.* **2013**, *423*, 55−61.

(27) Siwick, B. J.; Dwyer, J. R.; Jordan, R. E.; Miller, R. J. D. Ultrafast Electron Optics: Propagation Dynamics of Femtosecond Electron Packets. *J. Appl. Phys.* **2002**, *92*, 1643.

(28) Hellmann, S.; Rossnagel, K.; Marczynski-Bühlow, M.; Kipp, L. Vacuum Space-Charge Effects in Solid-State Photoemission. *Phys. Rev. B: Condens. Matter Mater. Phys.* **2009**, *79*, 035402.

(29) van der Geer, S. B.; de Loos, M. J. The Simulation Package Is General Particle Tracer (GPT). (http://www.pulsar.nl/gpt).

(30) Dwyer, J. R.; et al. Femtosecond Electron Diffraction: Making the Molecular Movie. *Philos. Trans. R. Soc., A* **2006**, *364*, 741−778.

(31) van der Geer, S. B.; de Loos, M. J.; Vredenbregt, E. J. D.; Luiten, O. J. Ultracold Electron Source for Single-Shot, Ultrafast Electron Diffraction. *Microsc. Microanal.* **2009**, *15*, 282−289.

(32) Ganter, R.; et al. Electron Beam Characterization of a Combined Diode RF Electron Gun. *Phys. Rev. Spec. Top.–Accel. Beams* **2010**, *13*, 093502.

(33) Kaufmann.; et al. Generation of Ultra-Short Hydrogen Atom Pulses by Bunch-Compression Photolysis. *Nat. Commun.* **2014**, *5*, 5373.

(34) Weiner, A. M. Femtosecond Pulse Shaping Using Spatial Light Modulators. *Rev. Sci. Instrum.* **2000**, *71*, 1929.

(35) Németh, K.; et al. High-Brightness Photocathodes through Ultrathin Surface Layers on Metals. *Phys. Rev. Lett.* **2010**, *104*, 046801.

DOI: 10.1021/acs.jpclett.5b01305
J. Phys. Chem. Lett. 2015, 6, 3867−3872

(36) Droubay, T. C.; et al. Metal-Insulator Photocathode Heterojunction for Directed Electron Emission. *Phys. Rev. Lett.* **2014**, *112*, 067601.
(37) Winkelmann, A.; et al. Direct k-Space Imaging of Mahan Cones at Clean and Bi-covered Cu(111) Surfaces. *New J. Phys.* **2012**, *14*, 083027.

DOI: 10.1021/acs.jpclett.5b01305
J. Phys. Chem. Lett. 2015, 6, 3867−3872